Muon $g-2$ and dark matter suggest nonuniversal gaugino masses: $SU(5)\times A_4$ case study at the LHC

Alexander S. Belyaev,[1,2,*] Steve F. King,[1,†] and Patrick B. Schaefers[1,‡]

[1]School of Physics and Astronomy, University of Southampton, Southampton SO17 1BJ, United Kingdom
[2]Particle Physics Department, Rutherford Appleton Laboratory, Chilton, Didcot, Oxon OX11 0QX, United Kingdom

(Received 25 January 2018; published 5 June 2018)

We argue that in order to account for the muon anomalous magnetic moment $g-2$, dark matter and LHC data, nonuniversal gaugino masses M_i at the high scale are required in the framework of the minimal supersymmetric standard model. We also need a right-handed smuon $\tilde{\mu}_R$ with a mass around 100 GeV, evading LHC searches due to the proximity of a neutralino $\tilde{\chi}_1^0$ several GeV lighter which allows successful dark matter. We discuss such a scenario in the framework of an $SU(5)$ grand unified theory (GUT) combined with A_4 family symmetry, where the three $\bar{5}$ representations form a single triplet of A_4 with a unified soft mass m_F, while the three 10 representations are singlets of A_4 with independent soft masses m_{T1}, m_{T2}, m_{T3}. Although m_{T2} (and hence $\tilde{\mu}_R$) may be light, the muon $g-2$ and relic density also requires light $M_1 \simeq 250$ GeV, which is incompatible with universal gaugino masses due to LHC constraints on M_2 and M_3 arising from gaugino searches. After showing that universal gaugino masses $M_{1/2}$ at the GUT scale are excluded by gluino searches, we provide a series of benchmarks which show that while $M_1 = M_2 \ll M_3$ is in tension with 8 and 13 TeV LHC data, $M_1 < M_2 \ll M_3$ is currently allowed. Even this scenario is almost excluded by the tension between the muon $g-2$, relic density, dark matter direct detection and LHC data. We focus on a region of parameter space that has not been studied in detail before being characterized by low Higgsino mass $\mu \approx -300$ GeV, as required by the muon $g-2$. The LHC will be able to fully test this scenario with the upgraded luminosity via muon-dominated tri- and dilepton signatures resulting from Higgsino-dominated $\tilde{\chi}_1^{\pm}\tilde{\chi}_2^0$ and $\tilde{\chi}_1^+\tilde{\chi}_1^-$ production.

DOI: 10.1103/PhysRevD.97.115002

I. INTRODUCTION

The minimal supersymmetric standard model (MSSM) remains an attractive candidate for physics beyond the standard model (BSM) even in the absence of any signal at the Large Hadron Collider (LHC). Despite the limits from direct and indirect searches for dark matter (DM), the lightest neutralino [1], whose stability is enforced by R parity, remains a prime candidate for the weakly interacting massive particle (WIMP).

There are several constraints from the LHC that restrict the parameter space of the MSSM, in particular, the requirement of a 125 GeV Higgs boson and stringent limits on the gluino mass [2,3].

An interesting possible signature of BSM physics is the muon $g-2$ or anomalous magnetic moment $a_\mu = (g-2)_\mu/2$ which differs from its standard model (SM) prediction by amount [4],

$$\Delta a_\mu \equiv a_\mu(\text{exp}) - a_\mu(\text{SM}) = (28.8 \pm 8.0) \times 10^{-10}. \quad (1)$$

Although it is possible to account for the muon $g-2$ within a supersymmetric framework [5–38], it is well known that it cannot be achieved in the MSSM with universal soft masses consistent with the above requirements, and therefore, some degree of nonuniversality is required. For example, nonuniversal gaugino masses have been shown to lead to an acceptable muon $g-2$ [25,27,31,39], while for a universal high-scale gaugino mass $M_{1,2} \neq M_3$ one is forced into a region of parameter space with large positive $\mu \sim 2$–5 TeV [37]. Based on fine-tuning considerations, one is motivated to consider smaller values of μ. In this paper we focus on successful regions of parameter space with $\mu \approx -300$ GeV, which have not been well studied hitherto.

It is well known that, to solve the muon $g-2$ problem in supersymmetry (SUSY) models, various mass spectra,

*A.Belyaev@soton.ac.uk
†S.F.King@soton.ac.uk
‡P.Schaefers@soton.ac.uk

including the general characteristics of the mass spectrum suggested in this paper, are preferred as discussed in the papers[5–38] mentioned above. It is worth giving a more detailed discussion about previous works, as well as the explanation of the difference between the previous works and the present one. In general the sensitive parameters for successful muon $g-2$ are the low-energy values of the Higgsino mass parameter μ, the bino soft mass M_1, the wino soft mass M_2, the smuon masses $m_{\tilde{\mu}_L}$ and $m_{\tilde{\mu}_R}$, the smuon neutrino mass $m_{\tilde{\nu}_\mu}$ and the ratio of Higgs vacuum expectation values $\tan\beta$. Some subset of these masses must be quite light, say of order 100 GeV, in order to explain the muon $g-2$. On the other hand there are stringent LHC limits on the colored sparticles, say of order 1 TeV. In addition some heavy stop squarks are required in order to obtain a sufficiently large Higgs mass around 125 GeV. A common way to achieve this is if, at the grand unified theory (GUT) scale, $M_3 \gg M_{1,2}$, which leads to all colored sparticles having large masses, while allowing at least some color singlet sparticles to remain light. This is also what we assume in this paper. However the novelty of our approach here is that we achieve this within the framework of an $SU(5)$ GUT with a particular flavor structure in which only one of the GUT matter representations, namely the second family 10 representation has a light soft mass $m_{T2} = 200$–300 GeV, leading to a light mass $m_{\tilde{\mu}_R} \sim 100$ GeV, with all other squarks contained in this representation gaining large mass from the large gluon corrections. All other GUT representations are assumed to have multi-TeV soft masses. The resulting low-energy sparticle spectrum involving only a light right-handed smuon, with all other squarks and sleptons being heavy, is one of the key distinguishing features of the present work.

In the framework of GUTs such as $SU(5)$ and $SO(10)$, nonuniversal gaugino masses at $M_{\rm GUT}$ can arise from specific nonsinglet F terms, or a linear combination of several such terms [40–47]. In general the gaugino masses come from the following dimension five term in the Lagrangian: $(\langle F_\Phi \rangle / M_{\rm Planck})\lambda_i\lambda_j$ where $\lambda_{1,2,3}$ are the $U(1)$, $SU(2)$ and $SU(3)$ gaugino fields (i.e., bino $\tilde{B}$, wino $\tilde{W}$ and gluino $\tilde{g}$, respectively). Since the gauginos belong to the adjoint representation of $SU(5)$, Φ and F_Φ can belong to any of the irreducible representations appearing in their symmetric product $(24\times 24)_{\rm sym} = 1+24+75+200$. If Φ is the singlet then this results in universal gaugino masses at the GUT scale. However if Φ belongs to one of the nonsinglet representations of $SU(5)$ then the gaugino masses are unequal, related to each other by the representation invariants. If several such Φ fields contribute in different representations then there is no longer any relation between the gaugino masses at the GUT scale. The most general situation is when all the gaugino masses may be considered as effectively independent. Recently, an $SU(5)$ model has been analyzed with completely nonuniversal gaugino masses and two universal soft masses, namely m_F and m_T, which accommodate the $\bar{5}$ and 10 representations, respectively (with the two Higgs soft masses set equal to m_F) [48]. In such a framework it was shown that the muon $g-2$ and dark matter may both be explained successfully. However, unlike our approach here, all $SU(5)$ $\bar{5}$ and 10 representations were assumed to have the same soft masses for all three families, while here we allow only the second family 10 to have a light soft mass, with all other representations having large soft masses, as discussed above.

In this paper, then, we argue that in order to account for the muon anomalous magnetic moment and dark matter in supersymmetry, in our studied region of parameter space for $\mu \approx -300$ GeV, nonuniversal gaugino masses are required. In particular, $M_{1,2} \ll M_3$, even for nonuniversal scalar masses. To achieve the desired pattern of nonuniversality, we consider an $SU(5)$ GUT combined with an A_4 family symmetry, where the three $\bar{5}$ representations form a single triplet of A_4 with a unified soft mass m_F, while the three 10 representations are singlets of A_4 with independent soft masses m_{T1}, m_{T2}, m_{T3}.[1] Assuming that $m_{T2} \ll m_{T1}, m_{T3}$, as discussed above, we show that it is not possible to account for the muon $g-2$ with universal gaugino masses. Allowing nonuniversal gaugino masses with $M_{1,2} \ll M_3$, we show that, with $\mu \approx -300$ GeV, it is possible to successfully explain both the muon anomalous magnetic moment and dark matter, while remaining consistent with all other experimental constraints. We present three benchmark points in our favored region of parameter space involving a right-handed smuon mass around 100 GeV, which can decay into a bino-dominated neutralino plus a muon. The remaining neutralino masses are all below about 300 GeV, while the rest of the SUSY spectrum has multi-TeV masses.

The layout of the remainder of the paper is as follows. In Sec. II, we present the $SU(5)\times A_4$ model and its symmetry breaking to the MSSM. In Sec. III, we summarize the MSSM one-loop contributions to Δa_μ and give first predictions for viable regions of parameter space of the model. All experimental constraints we take into account (both collider and cosmological constraints) are listed and explained in Sec. IV. In Sec. V, we present scans of the model parameter space for universal and nonuniversal gaugino masses, which also helps clarify the necessity of nonuniversal gaugino masses. Lastly, we draw our conclusions in Sec. VI.

II. THE MODEL

We first consider the gauge group $SU(5)$, which is rank 4 and has 24 gauge bosons which transform as the **24** adjoint representation. A left-handed lepton and quark fermion family is neatly accommodated into the $SU(5)$ representations $F = \bar{\mathbf{5}}$ and $T = \mathbf{10}$, where

[1] In this paper we ignore the induced off-diagonal elements of the sfermion mass matrices due to A_4 symmetry breaking, which become new sources of flavor violation. Such flavor violation has been studied in similar models based on $S_4 \times SU(5)$ and found to be quite suppressed and within experimental limits; for example see [49,50].

$$F=\begin{pmatrix} d_r^c \\ d_b^c \\ d_g^c \\ e^- \\ -\nu_e \end{pmatrix}_L, \quad T=\begin{pmatrix} 0 & u_g^c & -u_b^c & u_r & d_r \\ . & 0 & u_r^c & u_b & d_b \\ . & . & 0 & u_g & d_g \\ . & . & . & 0 & e^c \\ . & . & . & . & 0 \end{pmatrix}_L, \quad (2)$$

where r, b, g are quark colors and c denotes CP conjugated fermions.

The $SU(5)$ gauge group may be broken to the SM by a Higgs multiplet in the **24** representation developing a vacuum expectation value,

$$SU(5) \to SU(3)_C \times SU(2)_L \times U(1)_Y, \quad (3)$$

with

$$\bar{\mathbf{5}} = d^c(\bar{\mathbf{3}}, \mathbf{1}, 1/3) \oplus L(\mathbf{1}, \bar{\mathbf{2}}, -1/2), \quad (4)$$

$$\mathbf{10} = u^c(\bar{\mathbf{3}}, \mathbf{1}, -2/3) \oplus Q(\mathbf{3}, \mathbf{2}, 1/6) \oplus e^c(\mathbf{1}, \mathbf{1}, 1), \quad (5)$$

where (Q, u^c, d^c, L, e^c) is a complete quark and lepton SM family. Higgs doublets H_u and H_d, which break electroweak symmetry in a two Higgs doublet model, may arise from $SU(5)$ multiplets $H_{\mathbf{5}}$ and $H_{\bar{\mathbf{5}}}$, providing the color triplet components can be made heavy. This is known as the doublet-triplet splitting problem.

When A_4 family symmetry is combined with $SU(5)$, it is quite common to unify the three families of $\bar{5} \equiv F \equiv (d^c, L)$ into a triplet of A_4, with a unified soft mass m_F, while the three $10_i \equiv T_i \equiv (Q, u^c, e^c)_i$ representations are singlets of A_4 with independent soft masses m_{T1}, m_{T2}, m_{T3} [51–55]. For simplicity, we assume that at the GUT scale we have $m_F = m_{H_u} = m_{H_d}$, where m_{H_u} and m_{H_d} are the mass parameters of the MSSM Higgs doublets.

In the considered $SU(5) \times A_4$ model we then have the soft scalar masses,

$$\begin{aligned} m_F &= m_{\tilde{D}_i^c} = m_{\tilde{L}_i} = m_{H_u} = m_{H_d}, \\ m_{T1} &= m_{\tilde{Q}_1} = m_{\tilde{U}_1{}^c} = m_{\tilde{E}_1{}^c}, \\ m_{T2} &= m_{\tilde{Q}_2} = m_{\tilde{U}_2{}^c} = m_{\tilde{E}_2{}^c}, \\ m_{T3} &= m_{\tilde{Q}_3} = m_{\tilde{U}_3{}^c} = m_{\tilde{E}_3{}^c}. \end{aligned} \quad (6)$$

Notice that the stop mass parameters are completely contained in m_{T3}, while the right-handed smuon mass arises from m_{T2}, and so on.

III. MSSM ONE-LOOP CONTRIBUTIONS TO Δa_μ

The Feynman diagrams for the one-loop contributions to Δa_μ in the MSSM are shown in Fig. 1 with the respective expression for each diagram given by Eqs. (7a)–(7e) [15,24].

$$\Delta a_\mu^{(A)} = \left(\frac{M_1 \mu}{m_{\tilde{\mu}_L}^2 m_{\tilde{\mu}_R}^2}\right) \frac{\alpha_1}{4\pi} m_\mu^2 \tan\beta \cdot f_{\mathrm{N}}^{(A)}\left(\frac{m_{\tilde{\mu}_L}^2}{M_1^2}, \frac{m_{\tilde{\mu}_R}^2}{M_1^2}\right), \quad (7a)$$

$$\Delta a_\mu^{(B)} = -\left(\frac{1}{M_1 \mu}\right) \frac{\alpha_1}{4\pi} m_\mu^2 \tan\beta \cdot f_{\mathrm{N}}^{(B)}\left(\frac{M_1^2}{m_{\tilde{\mu}_R}^2}, \frac{\mu^2}{m_{\tilde{\mu}_R}^2}\right), \quad (7b)$$

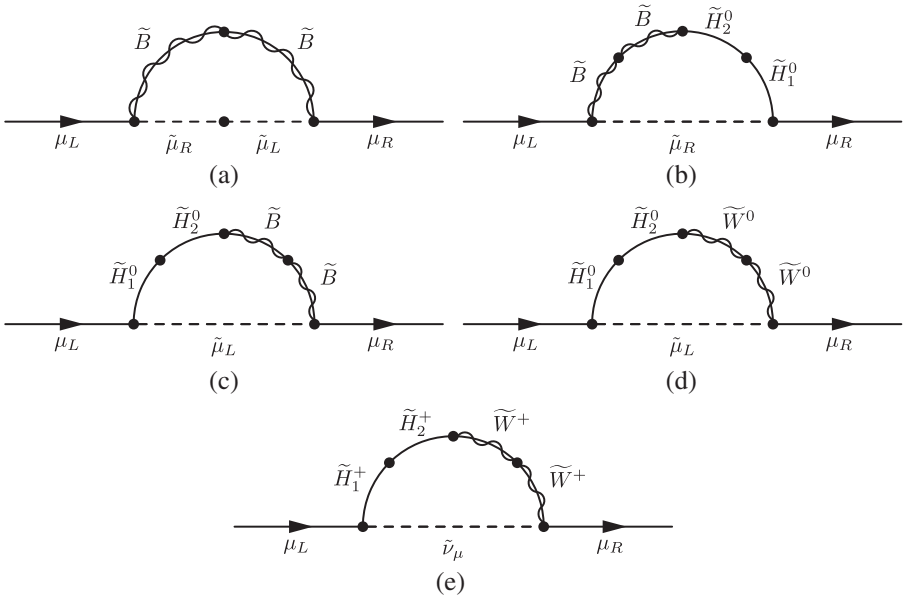

FIG. 1. One-loop contributions to the anomalous magnetic moment of the muon for supersymmetric models with low-scale MSSM.

$$\Delta a_\mu^{(C)} = \left(\frac{1}{M_1\mu}\right)\frac{\alpha_1}{8\pi}m_{\tilde{\mu}}^2\tan\beta\cdot f_{\rm N}^{(C)}\left(\frac{M_1^2}{m_{\tilde{\mu}_L}^2},\frac{\mu^2}{m_{\tilde{\mu}_L}^2}\right), \quad (7c)$$

$$\Delta a_\mu^{(D)} = -\left(\frac{1}{M_2\mu}\right)\frac{\alpha_2}{8\pi}m_{\tilde{\mu}}^2\tan\beta\cdot f_{\rm N}^{(D)}\left(\frac{M_2^2}{m_{\tilde{\mu}_L}^2},\frac{\mu^2}{m_{\tilde{\mu}_L}^2}\right), \quad (7d)$$

$$\Delta a_\mu^{(E)} = \left(\frac{1}{M_2\mu}\right)\frac{\alpha_2}{4\pi}m_{\tilde{\mu}}^2\tan\beta\cdot f_{\rm C}^{(E)}\left(\frac{M_2^2}{m_{\tilde{\nu}_\mu}^2},\frac{\mu^2}{m_{\tilde{\nu}_\mu}^2}\right). \quad (7e)$$

Here, α_1 and α_2 label the $U(1)_Y$ and $SU(2)_L$ fine structure constants respectively and the functions $f_{\rm N}^{(A,B,C,D)}(x,y)$ and $f_{\rm C}^{(E)}(x,y)$ are given by

$$f_{\rm N}^{(A,B,C,D)}(x,y) = xy\left[\frac{-3+x+y+xy}{(x-1)^2(y-1)^2}+\frac{2x\log x}{(x-y)(x-1)^3} - \frac{2y\log y}{(x-y)(y-1)^3}\right], \quad (8a)$$

$$f_{\rm C}^{(E)}(x,y) = xy\left[\frac{5-3(x+y)+xy}{(x-1)^2(y-1)^2}-\frac{2\log x}{(x-y)(x-1)^3} + \frac{2\log y}{(x-y)(y-1)^3}\right], \quad (8b)$$

where we use the superscripts (A,B,C,D) and (E) as a short notation to allow omission of the mass ratio arguments. Both f_N and f_C are monotonically increasing for all $0 \le (x,y) < \infty$ and are defined in $0 \le f_{N,C} \le 1$ [24].

One of the most important parameters influencing Δa_μ is μ, or rather $\operatorname{sgn}\mu$. Having positive μ means positive contributions from diagrams (A), (C) and (E), whereas negative μ results in (B) and (E) giving positive contributions to Δa_μ. Although it has been shown in the past that the constrained MSSM (cMSSM) with its usual five parameters ($M_{1/2}, m_0, \tan\beta, A_0, \operatorname{sgn}\mu$) is able to yield the observed Δa_μ, it cannot account simultaneously for further experimental limits (see e.g., [15,24,26]), regardless of $\operatorname{sgn}\mu$ but especially not for negative μ. Extending the cMSSM or relaxing some of its constraints changes the picture and new solutions without the need for fine-tuning arise—all while being in conformity with all other low-energy observations [5–17,19–38].

In this work, we focus on regions in model parameter space having viable Δa_μ for negative μ together with an especially light mass spectrum. Solutions with positive $\mu \sim$ 2–5 TeV are possible for a universal high-scale gaugino mass $M_{1,2} \neq M_3$ [37]. However, motivated by fine-tuning considerations, we focus on negative and small μ in the following. Negative μ infers that we are able to enhance the contribution from diagram (B) in which the right-handed smuons (but not the left-handed smuons) appear. As already mentioned, negative μ results in diagram (B) giving a positive contribution to Δa_μ and this is the main reason why we favor negative μ. In general, for negative μ, the contribution from diagrams (B) and (D) is enhanced, while all contributions from diagrams (A), (C) and (E) (see Sec. III) are simultaneously suppressed. Enhancing (B) and (D) requires small $|\mu|$ (not directly controllable), small M_1 and M_2 as well as light left- and right-handed smuon masses $m_{\tilde{\mu}_L}$ and $m_{\tilde{\mu}_R}$ (controlled by m_F or m_{T2} respectively). On the other hand, light $m_{\tilde{\mu}_L}$ would lead to unwanted large contributions from diagrams (A) and (C). This is one reason to not have light $m_{\tilde{\mu}_L}$, but makes them rather heavy. Another reason for heavy $m_{\tilde{\mu}_L}$ comes from the model parameter space itself. Since $m_{\tilde{\mu}_L}$ is governed by m_F, which also controls the muon sneutrino mass $m_{\tilde{\nu}_L^\mu}$ appearing in diagram (E), it is possible to decrease contributions from diagrams (A), (C) and (E) in one go by setting m_F large.

In the next section we briefly summarize the experimental constraints, before discussing the full results in detail in Sec. V.

IV. EXPERIMENTAL CONSTRAINTS

While the underlying model is proposed for the high-energy sector, it should nevertheless comprise any low-energy observations and limits coming from various experiments. In particular, we take into account the dark matter relic density, dark matter direct detection (DD) cross sections, the Higgs boson mass, constraints coming from $\mathrm{Br}(B_S \to \mu^+\mu^-)$ as well as $\mathrm{Br}(b \to s\gamma)$ and several 8 and 13 TeV ATLAS and CMS searches at the LHC. Regarding the DM relic density, the current combined best fit to data from PLANCK and WMAP is $\Omega h^2 = 0.1198 \pm 0.0026$ [56] and we consider a parameter space with $\Omega h^2 \lesssim 0.1224$.

The current best DM DD limit comes from the XENON1T experiment, reading $\sigma_{\text{DD-SI}} \le 7.64 \times 10^{-47}\,\mathrm{cm}^2 = 7.64 \times 10^{-11}\,\mathrm{pb}$ [57] for spin-independent models and a WIMP mass of 36 GeV. Since WIMP masses smaller or larger than 36 GeV lead to weaker limits, this choice is conservative. Concerning the Higgs boson mass, the current combined ATLAS and CMS measurement is $m_h = (125.09 \pm 0.21(\mathrm{stat.}) \pm 0.11(\mathrm{sys.}))$ GeV [58]. However, due to the theoretical error in the radiative corrections to the Higgs mass inherent in the existing state of the art SUSY spectrum generators, we consider instead the larger range $m_h = (125.09 \pm 1.5)$ GeV, which encompasses the much larger theoretical uncertainties. The branching ratios $\mathrm{Br}(b \to s\gamma) = (3.29 \pm 0.19 \pm 0.48) \times 10^{-4}$ [59] and $\mathrm{Br}(B_s \to \mu^+\mu^-) = 3.0^{+1.0}_{-0.9} \times 10^{-9}$ [60] are directly applied to our results.

V. RESULTS

Following the strategy to enhance Δa_μ in Sec. III and the experimental constraints in Sec. V, we are left with the following desired choice of parameters:

TABLE I. Input parameters at the GUT scale in GeV (apart for $\tan\beta$ and sgnμ) for universal gaugino masses $M_{1/2}$.

Parameter	m_F	m_{T1}	m_{T2}	m_{T3}	$M_{1/2}$	A_{tri}	$m_{H_{1,2}}$	$\tan\beta$	sgnμ
Value	6000	7000	300	free	free	−6000	6000	30	−1

TABLE II. Input parameters at the GUT scale in GeV for nonuniversal gaugino masses $M_{1,2}$ and M_3.

Parameter	m_F	m_{T1}	m_{T2}	m_{T3}	$M_{1,2}$	M_3	A_{tri}	$m_{H_{1,2}}$	$\tan\beta$	sgnμ
Value	6000	7000	300	free	250	free	−5000	6000	30	−1

(i) m_F large for large $m_{\tilde{\mu}_L}$ and $m_{\tilde{\nu}_L^{\mu}}$,
(ii) m_{T2} small for light $m_{\tilde{\mu}_R}$,
(iii) m_{T1} and m_{T3} large for large squark masses,
(iv) M_1 small for light $\tilde{\chi}_1^0$,
(v) $\tan\beta$ large (affects all diagrams).

All other parameters are, in principle, unconstrained, but in practice are constrained by experiment.

To gather the data for this work, we used `SPheno_v4.0.3` [61,62] to generate the mass spectra based on input points chosen randomly as well as on fixed grids with variable grid spacing in the parameter space from Tables I and II below. Subsequently, we employ `micrOMEGAs_v3.6.9.2` [63] to compute Δa_μ and the low-energy constraints listed in Sec. IV. In the following two subsections, we present scans taking these considerations into account. Section V A holds data and results regarding fully universal gaugino masses, commonly labeled as $M_{1/2}$, whereas Sec. V B refers to the case of partially nonuniversal gaugino masses, labeled as $M_{1,2}$ and M_3, and Sec. V C refers to the case of fully nonuniversal gaugino masses labeled M_1, M_2 and M_3.

A. Universal gaugino masses

The scan with universal gaugino masses $M_{1/2}$ was performed with

$$m_{T3} \in [200, 7000]\ \text{GeV},$$
$$M_{1/2} \in [200, 7000]\ \text{GeV}$$

and all other parameters fixed with values as shown in Table I. An overview over the scanned m_{T3}-$M_{1/2}$ plane is shown in Fig. 2, where the color coding indicates the value of Δa_μ. The first thing to notice is that only a narrow stripe in the parameter space leads to radiative electroweak symmetry breaking (REWSB). Following the stripe to larger m_{T3} and smaller $M_{1/2}$ gives larger Δa_μ, before the stripe eventually ends in a narrow peak around $(m_{T3}, M_3) = (5.3, 1.3)$ TeV. However, even in the peak Δa_μ only reaches values up to 1.8×10^{-10}, which is about 10–20 times lower than observed. Before giving an explanation for why Δa_μ is so small even with the assumptions made before, let us investigate the relic density and μ behavior shown in Fig. 3. Regarding the relic density

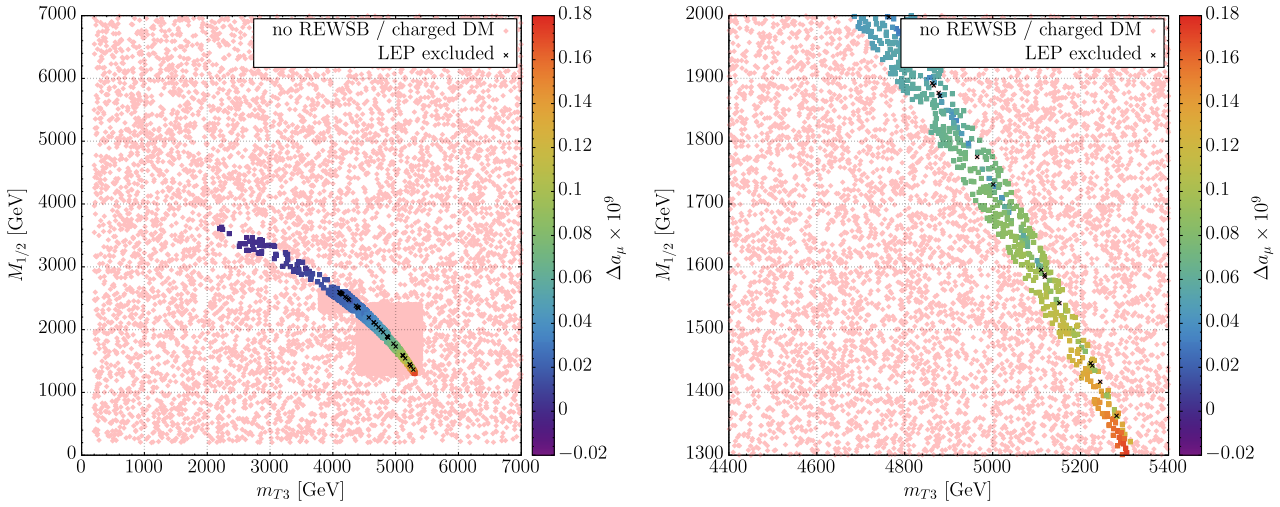

FIG. 2. m_{T3}-$M_{1/2}$ plane with color-coded Δa_μ with universal gaugino masses. The right panel is an excerpt of the full scan shown in the left panel.

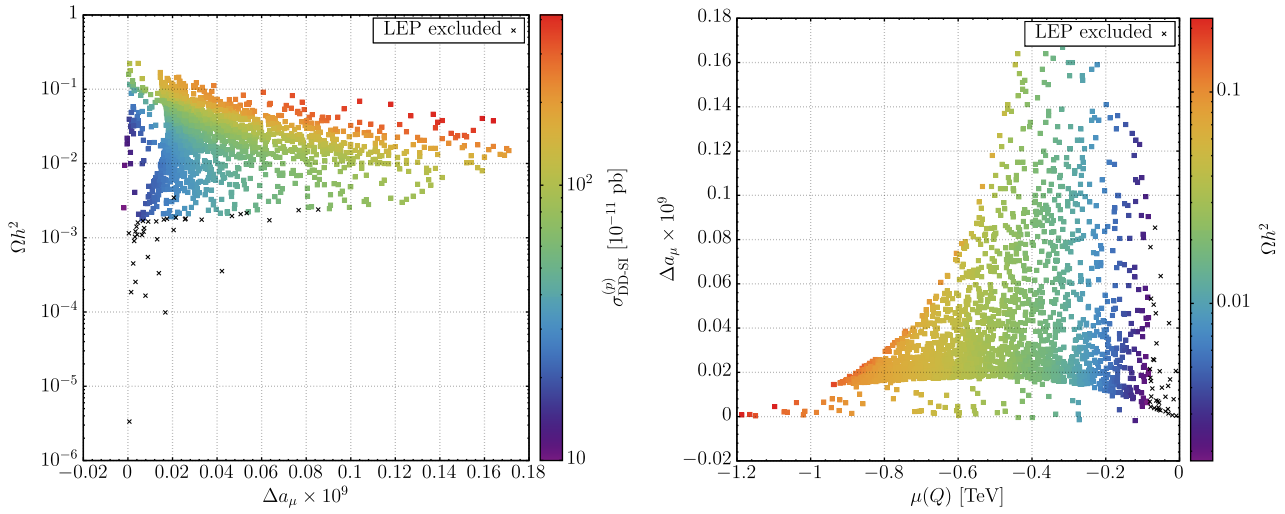

FIG. 3. Left: Relic density vs Δa_μ with color-coded $\sigma^{(p)}_{\text{DD-SI}}$ with universal gaugino masses. Right: Δa_μ vs μ with color-coded relic density Ωh^2 with universal gaugino masses.

shown in the left panel of Fig. 3, it turns out that DM is mostly Higgsino-like, thus yielding relic densities in the right range or maximally 2 orders of magnitude smaller than the observed upper limit. With increasing Δa_μ, the relic density slightly converges to some central value between its minimum and maximum reach. While the relic density thus is not a problem with this setup, the predicted DM DD cross sections turn out to be fully excluded (see color coding). This can be readily understood since dark matter in this case is dominantly Higgsino-like and therefore has a significant coupling to the Higgs boson, leading to a large DM DD cross section.

The right panel of Fig. 3 shows Δa_μ as a function of μ and it turns out that smaller values of μ yield larger values of Δa_μ, as was expected (see Sec. III and the beginning of this Sec. V). It is also worth noticing that decreasing μ results in a decreased relic density due to the DM becoming more and more Higgsino-like, as indicated by the color-coded Ωh^2.

In summary, the case of universal $M_{1/2}$ at the GUT scale with negative μ does not yield any values of Δa_μ in or close to the 1σ reference bound. This is expected and can be reasoned by the following argument. With negative μ, only Eqs. (7b) and (7d) give positive contributions to Δa_μ, while the major differences between (7b) and (7d) are simply the exchange of M_1 and M_2 as well as $m_{\tilde{\mu}_R}$ and $m_{\tilde{\mu}_L}$. Since the loop functions only run from 0 to 1, they are irrelevant for our argument and we can conservatively assume for the moment that they both equal 1 and consider just the remaining prefactors. With M_1 and M_2 unified at the GUT

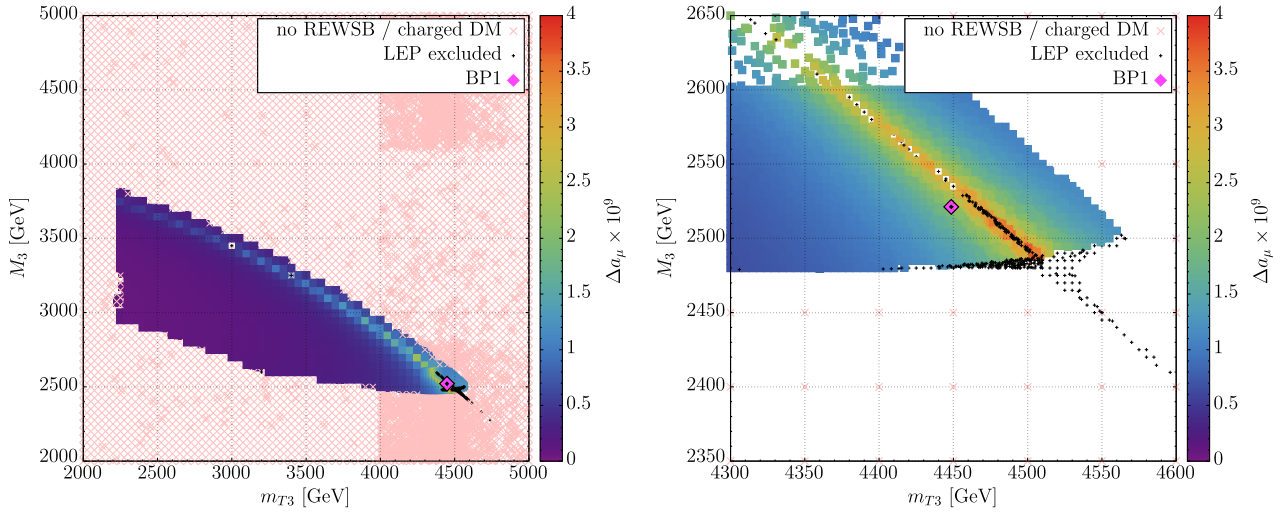

FIG. 4. m_{T3}-M_3 plane with color-coded Δa_μ with nonuniversal gaugino masses. The panel at the right is an excerpt of the full scan shown in the left panel.

scale, their low-scale values are not much different either and allow us to focus solely on one of the two equations, e.g., (7b). To get suitable Δa_μ, M_1 as well as μ need to be small [$\mathcal{O}(200)$ GeV]. However, having M_1 that light results in a similar light M_3 leading to light gluinos with masses $m_{\tilde{g}} \lesssim 1$ TeV [18] which are already excluded by LHC searches [2,3] as we have checked in our study. Additionally, too small $M_{1/2}$ prevents REWSB from happening, as can be seen in Fig. 2.

Overall, in the case of unified gaugino masses $M_{1/2}$, we did not find a region in parameter space able to explain Δa_μ in harmony with the other experimental constraints considered. However, a possible solution arises when the gaugino masses are split into $M_{1,2}$ and M_3, allowing for heavy gluinos and light enough $M_{1,2}$ to yield the correct Δa_μ. This setup is studied in detail in the following Sec. V B.

B. Partially nonuniversal gaugino masses

Splitting $M_{1/2}$ into $M_{1,2}$ and M_3 allows us to keep M_3 heavy, while fixing $M_{1,2}$ to some value light enough to strengthen rather than weaken Δa_μ. We performed a scan taking this into account with

$$m_{T3} \in [500, 7000] \text{ GeV},$$
$$M_3 \in [500, 7000] \text{ GeV}$$

and all other parameters fixed with values as shown in Table II. Analogous to Fig. 2, we show the scanned over

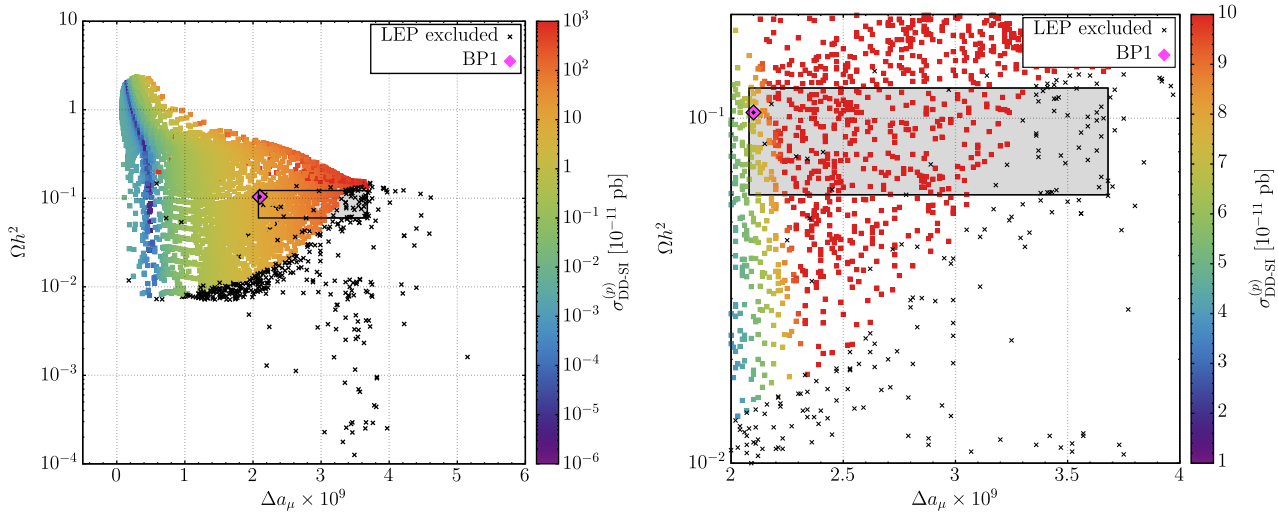

FIG. 5. Relic density vs Δa_μ with color-coded $\sigma^{(p)}_{\text{DD-SI}}$ with nonuniversal gaugino masses. The grey shaded rectangle shows the (extended) 1σ bound for Δa_μ (Ωh^2). The panel at the right is an excerpt of the full scan shown in the left panel.

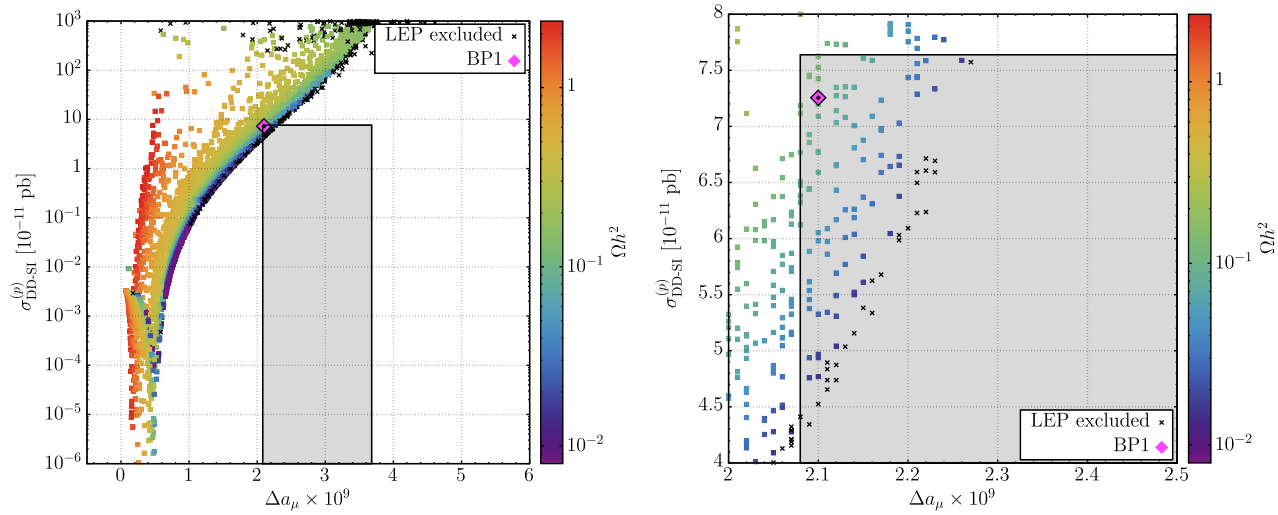

FIG. 6. $\sigma_{\text{DD-SI}}$ vs Δa_μ with color-coded relic density Ωh^2 with nonuniversal gaugino masses. The grey shaded rectangle shows the 1σ bound for Δa_μ and the upper limit for $\sigma_{\text{DD-SI}}$. The panel at the right is an excerpt of the full scan shown in the left panel.

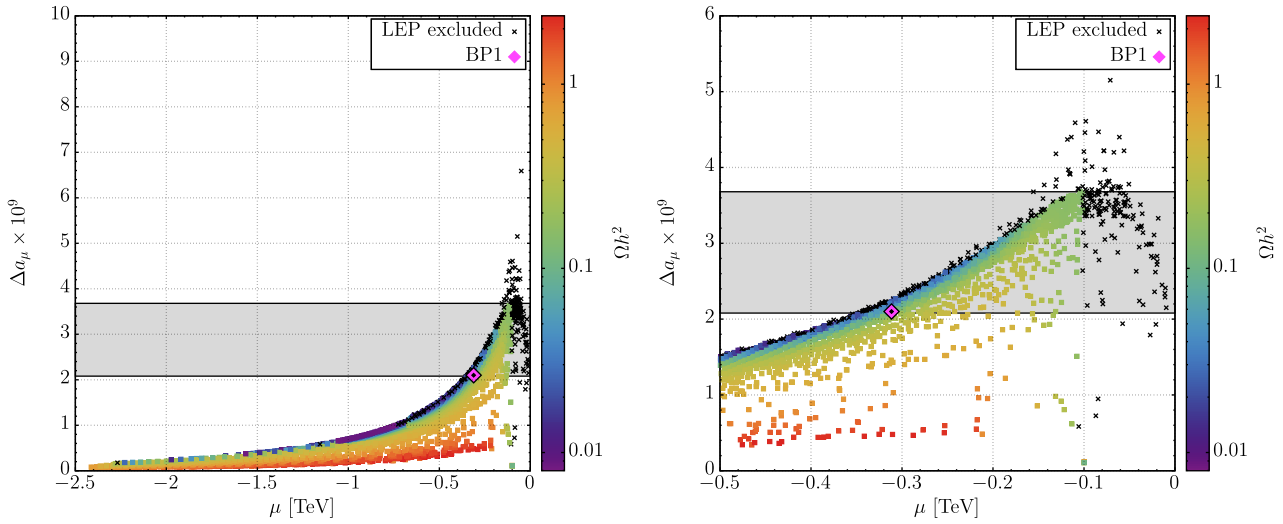

FIG. 7. Δa_μ vs μ with color-coded relic density Ωh^2 with nonuniversal gaugino masses. The grey shaded rectangle shows the 1σ bound for Δa_μ. The panel at the right is an excerpt of the full scan shown in the left panel.

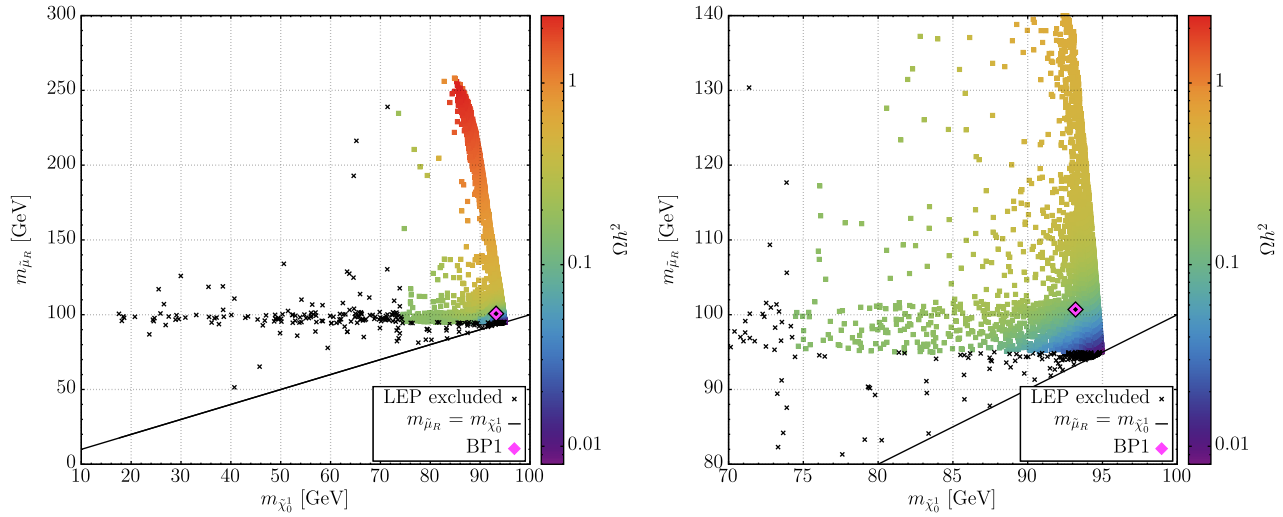

FIG. 8. $m_{\tilde{\mu}_R}$ vs $m_{\tilde{\chi}_1^0}$ with color-coded relic density Ωh^2 with nonuniversal gaugino masses. The panel at the right is an excerpt of the full scan shown in the left panel.

m_{T3}-M_3 plane in Fig. 4. Similar to the case of universal gaugino masses, a narrow, slightly elliptic stripe of solutions with larger Δa_μ can be seen for $M_3 \lesssim 3.8$ TeV and $m_{T3} \lesssim 4.5$ TeV. Additionally, a wide band around this stripe holds points where REWSB is happening, but Δa_μ is close to 0. A second set of points with vanishingly small Δa_μ is found for $M_3 \gtrsim 3$ TeV and $m_{T3} \gtrsim 6.5$ TeV (not shown here). When zooming in on the interesting part of the scan with larger values of Δa_μ (see the right panel of Fig. 4), we notice that the stripe extends into the nonphysical region without REWSB, although the points here are excluded by Large Electron-Positron Collider (LEP) limits due to too light charginos or smuons. Just before hitting the unphysical region, Δa_μ peaks at values around 4×10^{-9} before eventually vanishing abruptly in the non-REWSB region. Comparing these first results to the case with universal gaugino masses, the large increase in Δa_μ immediately becomes visible, therefore validating our assumptions made earlier.

In Fig. 5, we show the relic density-Δa_μ plane with color-coded DM direct detection cross sections, analogous to Fig. 3, left. This time, however, dark matter is mainly binolike and $\sigma_{\text{DD-SI}}$ is smaller than in Fig. 3 and increases faster with increasing Δa_μ. In the right panel of Fig. 5, a zoomed excerpt without logarithmic scaling[2] of $\sigma_{\text{DD-SI}}$ shows that most of the 1σ reference bounds for Δa_μ and Ωh^2 are excluded by DM direct detection, only leaving a

[2]To allow for an easier comparison in the relevant range of $\sigma_{\text{DD-SI}}$, i.e., approximately between 1×10^{-11} pb and 7.64×10^{-11} pb, values of $\sigma_{\text{DD-SI}} > 10 \times 10^{-11}$ pb are also colored red.

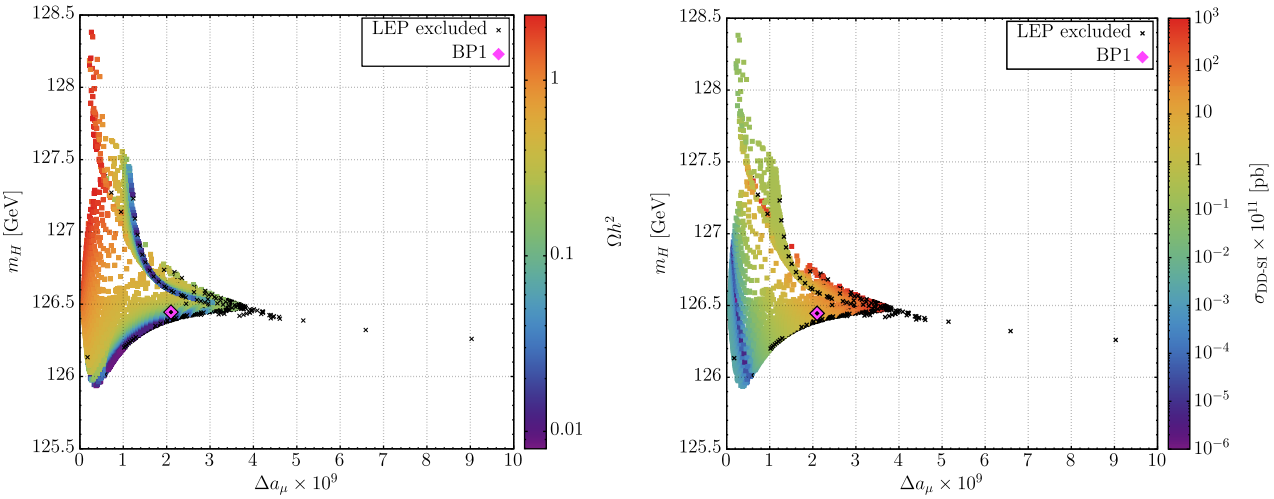

FIG. 9. m_h vs Δa_μ with color-coded Ωh^2 (left) and $\sigma_{\text{DD-SI}}$ (right) with nonuniversal gaugino masses.

small range of solutions for the lower edge of the Δa_μ 1σ bound. Nevertheless, in comparison to universal gaugino masses, there are solutions for nonuniversal gaugino masses that satisfy all experimental limits.

Similar to Figs. 5 and 6 holds the same data but with Ωh^2 and $\sigma_{\text{DD-SI}}$ switched. Presenting the data this way allows for a better understanding of the excluded and allowed parameter space with respect to $\sigma_{\text{DD-SI}}$. As can be seen in Fig. 6, right, only a small fraction of points falls within the 1σ reference bounds of Δa_μ and $\sigma_{\text{DD-SI}}$ (grey rectangle), although the majority of these points provide a very good relic density.

In Fig. 7, the μ dependence of Δa_μ is shown and it turns out that μ needs to be between -300 and -100 GeV in order to yield the desired Δa_μ. When μ goes closer to 0, the Higgsino components of the LSP start to dominate while simultaneously, the mass of the lightest chargino falls below approximately 100 GeV. Such light charginos are excluded by LEP [64], thus limiting our parameter space to values of μ smaller than -100 GeV.

In Fig. 8, we show the $m_{\tilde{\mu}_R}$-$m_{\tilde{\chi}_1^0}$ plane with color-coded relic density. As can be seen in the right panel, the pink benchmark point sits well above the line where the right-handed smuon and lightest supersymmetric particle (LSP) are mass degenerate. For this benchmark point, the LSP is predominantly binolike, but with a nonzero Higgsino component. This allows for a significant amount of $\tilde{\chi}_1^0$-$\tilde{\chi}_1^0$ annihilation in addition to the dominant $\tilde{\mu}_R$-$\tilde{\chi}_1^0$ coannihilation cross-section leading to the correct relic density.

In Fig. 9, we show the Higgs mass m_h as a function of Δa_μ with color-coded Ωh^2 (left) and $\sigma_{\text{DD-SI}}$ (right). For small values of Δa_μ, a broad range of Higgs masses is accessible with REWSB. This range shrinks drastically with increasing Δa_μ and eventually peaks at $m_h = 126.5$ GeV for $\Delta a_\mu \approx 4 \times 10^{-9}$. The relic density generally decreases with increasing Δa_μ, while the DM DD cross sections increase, as discussed before.

Lastly, in Fig. 10 in the right panel we show a comparison between Δa_μ as a function of $M_3(Q)$ (lower horizontal axis) and $m_{\tilde{g}}$ (top horizontal axis) for both universal (purple diamonds) and nonuniversal (orange squares) gaugino masses. It is clearly visible that universal gaugino masses cannot lead to viable Δa_μ and—even if there were a way to increase Δa_μ further—the gluinos would become quite light, potentially violating existing collider constraints. In the case of nonuniversal gaugino masses, the Δa_μ spectrum with respect to M_3 is slightly squeezed, but approximately 1 order of magnitude larger. This leads to a large spectrum of points

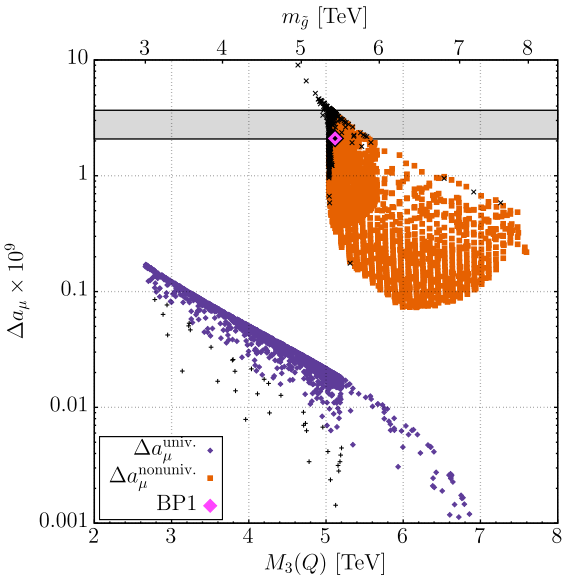

FIG. 10. Influence of having universal (nonuniversal) gaugino masses $M_{1/2}$ $(M_{1,2}, M_3)$ on Δa_μ. The purple (red) points represent the universal (nonuniversal) case. The grey shaded rectangle shows the 1σ bound for Δa_μ. Note that, to allow for an easier comparison, the nonuniversal points were gathered with $A_{\text{tri}} = -6$ TeV instead of $A_{\text{tri}} = -5$ TeV as shown for Figs. 4–8.

TABLE III. Input and output parameters for the benchmark points with partial gaugino nonuniversality $M_1 = M_2 \ll M_3$. These points have good Δa_μ as well as Ωh^2 but the wino dominated charginos $\tilde{\chi}_1^\pm$ and neutralinos $\tilde{\chi}_2^0$ are too light to have avoided 8 TeV LHC searches as discussed in the text. $\tilde{q}^i$ labels the i-th generation of squarks.

	Benchmark	BP1	BP2	BP3	
	$\tan\beta$	30	28	28	
	$\mathrm{sgn}(\mu)$	-1	-1	-1	
Input at GUT scale	m_F	6000.0	6000.0	6200.0	[GeV]
	m_{T1}	7000.0	6000.0	5700.0	
	m_{T2}	300.0	300.0	290.0	
	m_{T3}	4448.6	5572.0	5518.0	
	$M_{1,2}$	250.0	250.0	250.0	
	M_3	2521.2	2446.0	2790.0	
	M_{h_1}	6000.0	6000.0	6200.0	
	M_{h_2}	6000.0	6000.0	6200.0	
	A_{tri}	-5000.0	0	-500.0	
Masses	m_h	126.4	124.3	124.7	[GeV]
	$m_{\tilde{g}}$	5457.7	5280.9	5963.4	
	$m_{\tilde{q}_L^1}$	8248.5	7312.5	7433.2	
	$m_{\tilde{u}_R}$	8250.1	7316.9	7439.2	
	$m_{\tilde{q}_L^2}$	4350.1	4173.2	4764.6	
	$m_{\tilde{c}_R}$	4377.1	4198.9	4788.7	
	$m_{\tilde{b}_1}$	4866.7	5884.2	6162.0	
	$m_{\tilde{t}_1}$	3944.4	5068.5	5340.8	
	$m_{\tilde{t}_2}$	4875.0	5887.4	6165.7	
	$m_{\tilde{d}_R}$	7423.9	7320.6	7832.1	
	$m_{\tilde{s}_R}$	7423.8	7320.5	7831.9	
	$m_{\tilde{b}_2}$	6934.5	6947.4	7453.3	
	$m_{\tilde{e}_L}$	5987.1	5988.4	6188.8	
	$m_{\tilde{e}_R}$	7001.2	5999.3	5699.4	
	$m_{\tilde{\mu}_L}$	5986.5	5988.0	6188.3	
	$m_{\tilde{\mu}_R}$	100.7	95.6	95.4	
	$m_{\tilde{\tau}_1}$	3731.8	5175.0	5057.0	
	$m_{\tilde{\tau}_2}$	5737.5	5789.7	5989.0	
	$m_{\tilde{\chi}_1^0}$	93.2	91.1	89.2	
	$m_{\tilde{\chi}_2^0}$	169.4	163.6	158.7	
	$m_{\tilde{\chi}_3^0}$	-341.9	-336.2	-337.8	
	$m_{\tilde{\chi}_4^0}$	353.9	347.8	348.6	
	$m_{\tilde{\chi}_1^\pm}$	169.6	163.7	158.9	
	$m_{\tilde{\chi}_2^\pm}$	356.8	350.7	351.5	
	$m_{\tilde{\nu}_L^e}$	5986.1	5987.5	6187.8	
	$m_{\tilde{\nu}_L^\mu}$	5985.6	5987.0	6187.3	
	$m_{\tilde{\nu}_L^\tau}$	5736.8	5788.7	5988.1	
	Q	4287.9	5353.0	5609.8	
	μ	-311.5	-302.1	-299.5	
Constraints	$\mathrm{Br}(b \to s\gamma)$	3.40×10^{-4}	3.35×10^{-4}	3.34×10^{-4}	[pb]
	$\mathrm{Br}(B_s \to \mu^+\mu^-)$	3.03×10^{-9}	3.04×10^{-9}	3.04×10^{-9}	
	$\sigma^{\mathrm{DD\ SI}}$	7.23×10^{-11}	7.59×10^{-11}	6.89×10^{-11}	
	Ωh^2	1.04×10^{-1}	4.65×10^{-2}	7.55×10^{-2}	
	Δa_μ	2.10×10^{-9}	2.09×10^{-9}	2.09×10^{-9}	

TABLE IV. CheckMATE analysis results for the benchmarks of Table III with partial gaugino nonuniversality $M_1 = M_2 \ll M_3$.

Quantity	Unit	Benchmark BP1	BP2	BP3
$r_{\max}$		7.38	9.16	9.30
$\sqrt{s}$	TeV	8	8	8
Analysis		ATLAS_1402_7029	ATLAS_1402_7029	ATLAS_1402_7029
Signal region		SR0taua06	SR0taua02	SR0taua02
Ref.		[69]	[69]	[69]
σ_{LO}	pb	1.65	1.85	2.14
$\mathrm{BR}(\tilde{\chi}_2^0 \to \tilde{\mu}_R^{\pm}\mu^{\mp})$	%	99.4	99.4	99.7
$\mathrm{BR}(\tilde{\chi}_2^0 \to \bar{q}q\tilde{\chi}_1^0)$	%	0.4	0.4	0.2
$\mathrm{BR}(\tilde{\chi}_2^0 \to \ell^{\pm}\ell^{\mp}\tilde{\chi}_1^0)$	%	0.1	0.1	<0.1
$\mathrm{BR}(\tilde{\chi}_2^0 \to \bar{\nu}_\ell\nu_\ell\tilde{\chi}_1^0)$	%	<0.1	<0.1	<0.1
$\mathrm{BR}(\tilde{\chi}_1^{\pm} \to \bar{d}^{1,2}u^{1,2}\tilde{\chi}_1^0)$	%	45.4	40.2	47.9
$\mathrm{BR}(\tilde{\chi}_1^{\pm} \to \tilde{\mu}_R^{\pm}\nu_\mu)$	%	31.9	39.8	34.7
$\mathrm{BR}(\tilde{\chi}_1^{\pm} \to \ell^{\pm}\nu_\ell\tilde{\chi}_1^0)$	%	22.7	20.0	17.4
$\Delta m(\tilde{\chi}_1^{\pm}, \tilde{\mu}_R)$	GeV	68.9	67.9	63.5
$\Delta m(\tilde{\chi}_2^0, \tilde{\mu}_R)$	GeV	68.7	67.7	63.3
$\Delta m(\tilde{\mu}_R, \tilde{\chi}_1^0)$	GeV	7.5	6.6	6.2

with Δa_μ in the correct range while simultaneously keeping the gluinos fairly heavy. Overall, having nonuniversal gaugino masses allows for a variety of points with viable Δa_μ, which then can be tested further against other experimental constraints, as was shown above. Based on these findings, we provide three qualitatively different benchmark points, summarized in Table III below. BP2 differs from BP1 mainly in having $\tan\beta = 28$ and $A_{\mathrm{tri}} = 0$, whereas BP3 has a nonvanishing negative A_{tri} and split m_F and m_{T1}.

The benchmark points in this region are characterized by (a) bino-dominated $\tilde{\chi}_1^0$ LSP being the dark matter particle with a mass below about 100 GeV; (b) a next-to-lightest right-handed smuon $\tilde{\mu}_R$ with mass several GeV heavier; (c) wino-dominated $\tilde{\chi}_2^0$ and $\tilde{\chi}_1^{\pm}$ having a mass gap between them and $\tilde{\chi}_1^0$ of less than the Z or W boson masses respectively; (d) non-negligible $\tilde{\mu}_R - \tilde{\mu}_L$ mixing (enhanced by not-so-small values of $\tan\beta$) and respectively non-negligible $\tilde{\chi}_1^{\pm} \to \tilde{\mu}_R^{\pm}\nu_\mu$ decay branching fractions; (e) Higgsino-dominated $\tilde{\chi}_3^0$ and $\tilde{\chi}_2^{\pm}$ with masses below 400 GeV; and (f) all other SUSY partners having multi-TeV masses.

Such a specific spectrum of light electroweak gauginos and right-handed smuons predicts a rather characteristic signal at the LHC. The signal comes dominantly from $\tilde{\chi}_1^{\pm}\tilde{\chi}_2^0$ and $\tilde{\chi}_1^{+}\tilde{\chi}_1^{-}$-pair production followed by the dominant $\tilde{\chi}_2^0$ decay into a smuon which—in its turn—decays into a muon and DM. On the other hand, due to the non-negligible $\tilde{\mu}_R$-$\tilde{\mu}_L$ mixing mentioned above, the branching ratio for $\tilde{\chi}^{\pm} \to \tilde{\mu}_R^{\pm}\nu_\mu$ becomes comparable to the three-body decay $\tilde{\chi}_1^{\pm} \to f\bar{f}'\tilde{\chi}_1^0$ via a virtual W boson. This $\mathrm{Br}(\tilde{\chi}_1^{\pm} \to \tilde{\mu}^{\pm}\nu_\mu)$ can be substantial ($\simeq$30%–50%) because of the significant Higgsino component. The signal strength $m_{\tilde{\mu}^{\pm}}$ strongly depends on the $\tilde{\mu}_R$-$\tilde{\chi}_1^0$ mass gap and can be quite hidden if this mass gap is small (below a few GeV) since in this case the smuon decay products will be soft. The $\tilde{\chi}_2^0$ decay is characterized by the dominant $\tilde{\chi}_2^0 \to \tilde{\mu}_R\nu_\mu$ decay with not-so-soft leptons (the energy of which is independent of $\tilde{\mu}_R$-$\tilde{\chi}_1^0$ mass gap) providing a very important contribution to the leptonic signature. Thus, the only signature from the scenario under study is very specific and characterized by muon-dominated di- and trilepton signatures at the LHC.

We have performed a CheckMATE 2.0.11 [65] analysis on these three benchmark points, including all implemented 8 and 13 TeV ATLAS and CMS analyses on chargino and neutralino searches with a light smuon, and have verified that the LHC in fact is highly sensitive to this part of the parameter space. In particular, we used MadGraph 5.2.3.3 [66] linked to CheckMATE to generate 50000 events for SUSY final states consisting of $\tilde{\mu}_R^{\pm}$, $\tilde{\chi}_1^0$, $\tilde{\chi}_2^0$ as well as $\tilde{\chi}_1^{\pm}$. Next, PYTHIA 8.2.30 [67] was used to shower and hadronize the events and eventually CheckMATE together with Delphes 3.3.3 [68] was used to perform the event and detector analysis. While setting the same cuts as were used for the experimental analyses, the CheckMATE framework therefore allows us to examine whether given points in the parameter space are allowed or ruled out by current experimental searches. For all three benchmarks, the ATLAS search ATLAS_1402_7029 [69] aimed at three leptons plus missing E_T was most sensitive. The $r_{\max}$ value defined by [65]

$$r_{\max} = \frac{S - 1.64 \cdot \Delta S}{S95},$$

where S is the number of predicted signal events with its uncertainty ΔS and $S95$ is the experimental 95% upper limit

TABLE V. Input and output parameters for the benchmark points with full gaugino nonuniversality $M_1 < M_2 \ll M_3$. These points have good Δa_μ as well as Ωh^2 with all other constraints being fulfilled. In particular the Higgsino dominated charginos $\tilde{\chi}_1^\pm$ and neutralinos $\tilde{\chi}_2^0$ are heavy enough to have avoided current LHC searches, but are a target for future searches, as discussed in the text. $\tilde{q}^i$ labels the i-th generation of squarks.

	Benchmark	BP4	BP5	BP6	
	$\tan\beta$	30	28	30	
	$\mathrm{sgn}(\mu)$	-1	-1	-1	
Input at GUT scale	m_F	5000.0	6200.0	5000.0	[GeV]
	m_{T1}	5000.0	5700.0	5000.0	
	m_{T2}	200.0	280.0	200.0	
	m_{T3}	2995.0	5430.0	3005.0	
	M_1	250.0	250.0	250.0	
	M_2	400.0	550.0	500.0	
	M_3	2600.0	2945.0	2595.0	
	M_{h_1}	5000.0	6200.0	5000.0	
	M_{h_2}	5000.0	6200.0	5000.0	
	A_{tri}	-4000.0	-500.0	-4000.0	
Masses	m_h	126.3	124.7	126.2	[GeV]
	$m_{\tilde{g}}$	5531.7	6235.3	5516.5	
	$m_{\tilde{q}_L^1}$	6743.0	7589.2	6735.7	
	$m_{\tilde{u}_R}$	6743.7	7589.9	6734.1	
	$m_{\tilde{q}_L^2}$	4516.4	5003.3	4505.7	
	$m_{\tilde{c}_R}$	4529.2	5018.0	4514.9	
	$m_{\tilde{b}_1}$	4312.4	6262.8	4306.4	
	$m_{\tilde{t}_1}$	3601.6	5443.3	3588.2	
	$m_{\tilde{t}_2}$	4324.0	6266.7	4318.0	
	$m_{\tilde{d}_R}$	6748.0	7975.4	6738.4	
	$m_{\tilde{s}_R}$	6747.9	7975.3	6738.3	
	$m_{\tilde{b}_2}$	6348.2	7597.3	6337.5	
	$m_{\tilde{e}_L}$	4994.9	6196.1	4998.5	
	$m_{\tilde{e}_R}$	5002.1	5699.9	5002.1	
	$m_{\tilde{\mu}_L}$	4994.4	6195.6	4998.0	
	$m_{\tilde{\mu}_R}$	98.9	96.8	99.4	
	$m_{\tilde{\tau}_1}$	2282.9	4968.1	2293.7	
	$m_{\tilde{\tau}_2}$	4802.1	5999.4	4805.3	
	$m_{\tilde{\chi}_1^0}$	91.7	89.0	92.0	
	$m_{\tilde{\chi}_2^0}$	266.9	303.3	302.2	
	$m_{\tilde{\chi}_3^0}$	-335.1	-327.8	-335.9	
	$m_{\tilde{\chi}_4^0}$	376.8	458.9	430.4	
	$m_{\tilde{\chi}_1^\pm}$	267.4	303.7	302.8	
	$m_{\tilde{\chi}_2^\pm}$	378.2	459.0	430.7	
	$m_{\tilde{\nu}_L^e}$	4993.8	6195.1	4997.4	
	$m_{\tilde{\nu}_L^\mu}$	4993.4	6194.6	4997.0	
	$m_{\tilde{\nu}_L^\tau}$	4800.9	5998.4	4804.1	
	Q	3866.1	5705.8	3856.5	
	μ	-313.0	-293.3	-314.3	
Constraints	$\mathrm{Br}(b \to s\gamma)$	3.43×10^{-4}	3.34×10^{-4}	3.43×10^{-4}	[pb]
	$\mathrm{Br}(B_s \to \mu^+\mu^-)$	3.01×10^{-9}	3.04×10^{-9}	3.01×10^{-9}	
	$\sigma^{\mathrm{DD\,SI}}$	6.72×10^{-11}	6.81×10^{-11}	6.52×10^{-11}	
	Ωh^2	9.67×10^{-2}	1.10×10^{-1}	1.03×10^{-1}	
	Δa_μ	2.17×10^{-9}	2.14×10^{-9}	2.16×10^{-9}	

TABLE VI. CheckMATE analysis results for the benchmarks of Table V with full gaugino nonuniversality $M_1 < M_2 \ll M_3$.

Quantity	Unit	Benchmark		
		BP4	BP5	BP6
$r_{\max}$		0.88	0.12	0.13
$\sqrt{s}$	TeV	13	13	13
Analysis		ATLAS_CONF_2016_096	ATLAS_CONF_2016_096	ATLAS_CONF_2016_096
Signal region		3LI	2LADF	3LI
Ref.		[70]	[70]	[70]
σ_{LO}	pb	0.54	0.24	0.26
$\mathrm{BR}(\tilde{\chi}_2^0 \to h\tilde{\chi}_1^0)$	%	51.0	55.5	55.4
$\mathrm{BR}(\tilde{\chi}_2^0 \to Z\tilde{\chi}_1^0)$	%	30.5	30.2	30.1
$\mathrm{BR}(\tilde{\chi}_2^0 \to \tilde{\mu}_R^{\pm}\mu^{\mp})$	%	18.5	14.3	14.5
$\mathrm{BR}(\tilde{\chi}_1^{\pm} \to W^{\pm}\tilde{\chi}_1^0)$	%	99.4	99.5	99.5
$\mathrm{BR}(\tilde{\chi}_1^{\pm} \to \tilde{\mu}_R^{\pm}\nu_{\mu})$	%	0.6	0.5	0.5
$\Delta m(\tilde{\chi}_1^{\pm}, \tilde{\mu}_R)$	GeV	168.5	207.0	203.4
$\Delta m(\tilde{\chi}_2^0, \tilde{\mu}_R)$	GeV	168.0	206.5	202.7
$\Delta m(\tilde{\mu}_R, \tilde{\chi}_1^0)$	GeV	7.2	7.8	7.5

on the number of signal events, is shown below in Table IV for all three benchmarks. Values of $r_{\max} \geq 1$ indicate the signal is excluded, whereas $r_{\max} < 1$ indicates that the signal is not excluded or probed yet.

It turns out that all benchmarks are strongly excluded, which is mainly due to the light $\tilde{\chi}_1^{\pm}$ and $\tilde{\chi}_2^0$ and their subsequent decays to the right-handed smuon.

A summary of the most powerfully excluding LHC searches for BP1—BP3 is given in Table IV, where we present the $r_{\max}$ value from CheckMATE together with properties of the principal decay channels for $\tilde{\chi}_1^{\pm}$ and $\tilde{\chi}_2^0$. The most sensitive search is actually done by ATLAS for the 8 TeV data ATLAS_1402_7029 [69] and the most sensitive signature is the trilepton one, containing always one soft muon from the $\tilde{\mu}_R \to \tilde{\chi}_1^0\mu$ decay. Even though this muon is soft, the well-designed asymmetric p_T cuts for the leptons in Ref. [69] allow for being sensitive to a second or third lepton with p_T as low as 10 GeV. To the best of our knowledge, analogue 13 TeV searches are not sensitive to such low p_T leptons.

C. Fully nonuniversal gaugino masses

So far, in the previous subsections we have shown that our scenario for the muon $g-2$ requires a light right-handed smuon around 100 GeV together with a neutralino several GeV lighter leading to successful dark matter. We have seen that such a scenario is not consistent with universal gauginos at the GUT scale due to the gluino mass bound, which requires $M_{1,2} \ll M_3$. We have also seen that this scenario is not consistent with $M_1 = M_2$ in the case of negative μ due to the subsequent prediction of wino-dominated charginos and neutralinos with masses around 160–170 GeV, which are excluded by 8 TeV LHC searches that are most sensitive for the resulting soft muons arising from smuon decays. For solutions with positive μ such as in Ref. [37], the overall mass spectrum is slightly heavier and lies outside the sensitivity reach of the 8 TeV LHC.[3]

In this section, we show that, allowing fully nonuniversal gaugino masses with $M_1 < M_2 \ll M_3$ gives charginos and neutralinos which are somewhat heavier, thereby satisfying current LHC search constraints. With such full nonuniversality, we may then access regions of parameter space where M_2 exceeds the magnitude of the Higgsino mass parameter (typically $\mu \sim -300$ GeV as required to achieve a successful muon $g-2$). Then the charginos and neutralinos become Higgsino-dominated with masses governed by $|\mu| \sim 300$ GeV. The full scans of the parameter space are quite analogous to those in the previous subsection, with the only difference being that M_2 is somewhat heavier than M_1. Therefore it suffices to present a few new benchmark points to illustrate the effect of having $M_1 < M_2 \ll M_3$.

In Table V, we define three new benchmark points BP4–BP6, corresponding to having $M_1 < M_2 \ll M_3$. The benchmark points in this region are characterized by (a) bino-dominated $\tilde{\chi}_1^0$ LSP being the dark matter particle with a mass below about 100 GeV; (b) a next-to-lightest right-handed smuon $\tilde{\mu}_R$ with a mass several GeV heavier; (c) Higgsino-dominated $\tilde{\chi}_2^0$ and $\tilde{\chi}_1^{\pm}$ with masses governed by $|\mu| \sim 300$ GeV; (d) wino-dominated $\tilde{\chi}_3^0$ and $\tilde{\chi}_2^{\pm}$ with masses governed by M_2; and (e) all other SUSY partners having multi-TeV masses.

The main difference from the previous benchmarks is that the wino-dominated charginos and neutralinos are now pushed up in mass due to the increase in M_2. However, the

[3]13 TeV searches, however, are anticipated to probe the solutions with positive μ [37].

remaining Higgsino-dominated charginos and neutralinos whose mass is governed by $|\mu|$ cannot be pushed up beyond $\simeq$300 GeV, since we need $\mu \sim -300$ GeV to achieve a successful muon $g-2$. These charginos and neutralinos therefore remain a target for LHC searches. We have again performed a `CheckMATE 2.0.11` analysis on these three benchmark points, including all implemented 8 and 13 TeV ATLAS and CMS analyses on chargino and neutralino searches with a light smuon and have verified that the LHC in fact is highly sensitive to this part of the parameter space. Following the procedure described in detail in the previous subsection, we have obtained the results shown in Table VI for all three benchmarks. Contrary to the previous results, now we see that all three benchmark points are consistent with current LHC searches; however BP4 is on the verge of being excluded with a value of $r_{\max} = 0.88$, while BP5 and BP6 both have $r_{\max} \approx 0.12$ and require a substantial increase in luminosity to exclude them. The search channels are di- and trilepton searches plus missing energy, as before, but since the chargino and neutralino masses are larger, the cross sections are now lower, as can be seen in Table VI.

Another reason why the sensitivity of the LHC to BP4 – BP6 is lower in comparison to the BP1 – BP3 case is because of the new decay channel $\tilde{\chi}_2^0 \to h\tilde{\chi}_1^0$ to which the current LHC searches have lower sensitivity. One can see from Table VI that the branching ratio to this channel is substantial (about 50%), which eventually further lowers the LHC sensitivity. One should also note that BP5 and BP6 represent the region of the parameter space to which the LHC is currently the least sensitive. Nevertheless, with a future total integrated luminosity of about 3 ab^{-1}, the LHC will be able to probe even these corners of the parameter space with di- and trilepton signatures from Higgsino production. Moreover, the increase of sensitivity of the DM direct detection experiments by a factor of 2, which is expected to take place in the next few years, will independently probe the entire parameter space of the scenario under study.

VI. CONCLUSIONS

In this paper, we have focused on a region of parameter space that has not been studied in detail before characterized by a Higgsino mass $\mu \approx -300$ GeV, as required by the muon $g-2$. In this region of parameter space, we have argued that in order to account for the muon anomalous magnetic moment $g-2$, dark matter and LHC data, nonuniversal gaugino masses with $M_1 \simeq 250$ GeV $< M_2 \ll M_3$ at the high scale are required in the framework of the MSSM. We also require a right-handed smuon $\tilde{\mu}_R$ with a mass around 100 GeV with a small mass gap to neutralino $\tilde{\chi}_1^0$ to evade LHC searches. The bino-dominated neutralino is a good dark matter candidate due to the presence of the nearby right-handed smuon with which it can efficiently coannihilate in the early Universe. However, the direct detection limits provided by XENON1T provide a strong constraint on this scenario.

We have discussed such a scenario in the framework of an $SU(5)$ GUT combined with A_4 family symmetry, where the three $\bar{5}$ representations form a single triplet of A_4 with a unified soft mass m_F, while the three 10 representations are singlets of A_4 with independent soft masses m_{T1}, m_{T2}, m_{T3}. Although m_{T2} (and hence $\tilde{\mu}_R$) may be light, the muon $g-2$ also requires $M_1 \simeq 250$ GeV which we have shown to be incompatible with universal gaugino masses at the GUT scale due to LHC constraints on M_2 and M_3 arising from gaugino searches. Therefore, we have allowed nonuniversal gaugino masses at the GUT scale, which is theoretically allowed in $SU(5)$ with nonsinglet F terms. One should stress that this model is representative of a larger class of such nonuniversal MSSM scenarios, which can give nonuniversal masses to left- and right-handed sfermions and which in particular allow a light right-handed smuon with mass around 100 GeV. After showing that universal gaugino masses $M_{1/2}$ at the GUT scale are excluded by gluino searches, we have provided a series of benchmarks which demonstrate that while $M_1 = M_2 \ll M_3$ for sgn$\mu = -1$ is also excluded by chargino searches, $M_1 < M_2 \ll M_3$ is currently allowed. However, there is an unavoidable prediction of our scenario, namely that the muon $g-2$ also requires a Higgsino mass $\mu \approx -300$ GeV, which—although consistent with current LHC searches for such Higgsino-dominated charginos and neutralinos—will be a target for future such searches. Although the wino-dominated charginos and neutralinos are expected to be somewhat heavier and the rest of the SUSY spectrum may have multi-TeV masses outside the reach of the LHC, the Higgsinos with mass of about 300 GeV cannot escape LHC searches, since they may be pair produced and decay to yield muon-dominated di- and trilepton plus missing transverse momentum signatures, which will be fully probed by the planned increase of total integrated luminosity of up to 3 ab^{-1}. Moreover, the increase of sensitivity of the DM direct detection experiments by a factor of 2, which is expected to take place in the next few years, will independently probe the entire parameter space of the scenario under study.

To conclude, if the muon $g-2$ turns out to be a true signal of new physics, then in our scenario we expect a right-handed smuon with mass around 100 GeV, with bino-dominated neutralino DM a few GeV lighter, and a Higgsino mass $\mu \approx -300$ GeV. The *whole* such region of MSSM parameter space could be effectively probed in the near future and either discovered or excluded by the combined LHC, relic density and DM direct detection experiments as we have discussed above.

ACKNOWLEDGMENTS

The authors acknowledge the use of the IRIDIS High Performance Computing Facility, and associated support services at the University of Southampton, in the

completion of this work. A. S. B., S. F. K. and P. B. S. acknowledge partial support from the InvisiblesPlus RISE from the European Union Horizon 2020 research and innovation program under the Marie Sklodowska-Curie Grant No. 690575. S. F. K. acknowledges partial support from the Elusives ITN from the European Union Horizon 2020 research and innovation program under the Marie Sklodowska-Curie Grant No. 674896. A. S. B. and Institute for Basic Science S. F. K. acknowledges partial support from the STFC Grant No. ST/L000296/1. A. S. B. also thanks the NExT Institute, Royal Society Leverhulme Trust Senior Research Fellowship Grant No. LT140094, Royal Society International Exchange Grant No. IE150682 and the Soton-FAPESP grant. A. S. B. also acknowledges the support of the IBS center in Daejeon for the hospitality and support.

[1] G. Jungman, M. Kamionkowski, and K. Griest, Supersymmetric dark matter, Phys. Rep. **267**, 195 (1996).
[2] ATLAS Collaboration, Search for pair-production of gluinos decaying via stop and sbottom in events with b-jets and large missing transverse momentum in $\sqrt{s} = 13$ TeV pp collisions with the ATLAS detector, CERN Report No. ATLAS-CONF-2015-067, 2015.
[3] A. M. Sirunyan *et al.* (CMS Collaboration), Search for new phenomena with the M_{T2} variable in the all-hadronic final state produced in proton-proton collisions at $\sqrt{s} = 13$ TeV, Eur. Phys. J. C **77**, 710 (2017).
[4] K. A. Olive *et al.* (Particle Data Group Collaboration) Review of particle physics, Chin. Phys. C **38**, 090001 (2014).
[5] A. S. Belyaev, J. E. Camargo-Molina, S. F. King, D. J. Miller, A. P. Morais, and P. B. Schaefers, A to Z of the muon anomalous magnetic moment in the MSSM with Pati-Salam at the GUT scale, J. High Energy Phys. 06 (2016) 142.
[6] J. A. Grifols and A. Mendez, Constraints on supersymmetric particle masses From $(g-2)$ μ, Phys. Rev. D **26**, 1809 (1982).
[7] J. R. Ellis, J. S. Hagelin, and D. V. Nanopoulos, Spin 0 leptons and the anomalous magnetic moment of the muon, Phys. Lett. **116B**, 283 (1982).
[8] J. Chakrabortty, S. Mohanty, and S. Rao, Nonuniversal gaugino mass GUT models in the light of dark matter and LHC constraints, J. High Energy Phys. 02 (2014) 074.
[9] J. Chakrabortty, A. Choudhury, and S. Mondal, Nonuniversal Gaugino mass models under the lamppost of muon $(g-2)$, J. High Energy Phys. 07 (2015) 038.
[10] R. Barbieri and L. Maiani, The muon anomalous magnetic moment in broken supersymmetric theories, Phys. Lett. **117B**, 203 (1982).
[11] D. A. Kosower, L. M. Krauss, and N. Sakai, Low-energy supergravity and the anomalous magnetic moment of the muon, Phys. Lett. **133B**, 305 (1983).
[12] T. C. Yuan, R. L. Arnowitt, A. H. Chamseddine, and P. Nath, Supersymmetric electroweak effects on G-2 (mu), Z. Phys. C **26**, 407 (1984).
[13] J. C. Romao, A. Barroso, M. C. Bento, and G. C. Branco, Flavor violation in supersymmetric theories, Nucl. Phys. **B250**, 295 (1985).
[14] J. L. Lopez, D. V. Nanopoulos, and X. Wang, Large $(g-2)$-mu in $SU(5) \times U(1)$ supergravity models, Phys. Rev. D **49**, 366 (1994).
[15] T. Moroi, The muon anomalous magnetic dipole moment in the minimal supersymmetric standard model, Phys. Rev. D **53**, 6565 (1996); Erratum, Phys. Rev. D **56**, 4424(E) (1997).
[16] S. P. Martin and J. D. Wells, Constraints on ultraviolet stable fixed points in supersymmetric gauge theories, Phys. Rev. D **64**, 036010 (2001).
[17] A. Czarnecki and W. J. Marciano, The muon anomalous magnetic moment: A harbinger for new physics, Phys. Rev. D **64**, 013014 (2001).
[18] H. Baer, A. Belyaev, T. Krupovnickas, and A. Mustafayev, SUSY normal scalar mass hierarchy reconciles $(g-2)_\mu$, $b \to s\gamma$ and relic density, J. High Energy Phys. 06 (2004) 044.
[19] G.-C. Cho, K. Hagiwara, Y. Matsumoto, and D. Nomura, The MSSM confronts the precision electroweak data and the muon $g-2$, J. High Energy Phys. 11 (2011) 068.
[20] M. Endo, K. Hamaguchi, S. Iwamoto, and N. Yokozaki, Higgs mass and muon anomalous magnetic moment in supersymmetric models with vectorlike matters, Phys. Rev. D **84**, 075017 (2011).
[21] M. Endo, K. Hamaguchi, S. Iwamoto, and N. Yokozaki, Higgs mass, muon $g-2$, and LHC prospects in gauge mediation models with vectorlike matters, Phys. Rev. D **85**, 095012 (2012).
[22] M. Endo, K. Hamaguchi, S. Iwamoto, K. Nakayama, and N. Yokozaki, Higgs mass and muon anomalous magnetic moment in the U(1) extended MSSM, Phys. Rev. D **85**, 095006 (2012).
[23] J. L. Evans, M. Ibe, S. Shirai, and T. T. Yanagida, A 125 GeV Higgs boson and muon $g-2$ in more generic gauge mediation, Phys. Rev. D **85**, 095004 (2012).
[24] M. Endo, K. Hamaguchi, S. Iwamoto, and T. Yoshinaga, Muon $g-2$ vs LHC in supersymmetric models, J. High Energy Phys. 01 (2014) 123.
[25] S. Mohanty, S. Rao, and D. P. Roy, Reconciling the muon $g-2$ and dark matter relic density with the LHC results in nonuniversal gaugino mass models, J. High Energy Phys. 09 (2013) 027.
[26] M. Ibe, T. T. Yanagida, and N. Yokozaki, Muon $g-2$ and 125 GeV Higgs in split-family supersymmetry, J. High Energy Phys. 08 (2013) 067.
[27] S. Akula and P. Nath, Gluino-driven radiative breaking, Higgs boson mass, muon $g-2$, and the Higgs diphoton decay in supergravity unification, Phys. Rev. D **87**, 115022 (2013).

[28] N. Okada, S. Raza, and Q. Shafi, Particle spectroscopy of supersymmetric SU(5) in light of 125 GeV Higgs and muon $g-2$ data, Phys. Rev. D **90**, 015020 (2014).
[29] M. Endo, K. Hamaguchi, T. Kitahara, and T. Yoshinaga, Probing bino contribution to muon $g-2$, J. High Energy Phys. 11 (2013) 013.
[30] G. Bhattacharyya, B. Bhattacherjee, T. T. Yanagida, and N. Yokozaki, A practical GMSB model for explaining the muon $(g-2)$ with gauge coupling unification, Phys. Lett. B **730**, 231 (2014).
[31] I. Gogoladze, F. Nasir, Q. Shafi, and C. S. Un, Nonuniversal gaugino masses and muon $g-2$, Phys. Rev. D **90**, 035008 (2014).
[32] J. Kersten, J.-h. Park, D. Stöckinger, and L. VelascoSevilla, Understanding the correlation between $(g-2)_\mu$ and $\mu \to e\gamma$ in the MSSM, J. High Energy Phys. 08 (2014) 118.
[33] T. Li and S. Raza, Electroweak supersymmetry from the generalized minimal supergravity model in the MSSM, Phys. Rev. D **91**, 055016 (2015).
[34] W.-C. Chiu, C.-Q. Geng, and D. Huang, Correlation between muon $g-2$ and $\mu \to e\gamma$, Phys. Rev. D **91**, 013006 (2015).
[35] M. Badziak, Z. Lalak, M. Lewicki, M. Olechowski, and S. Pokorski, Upper bounds on sparticle masses from muon $g-2$ and the Higgs mass and the complementarity of future colliders, J. High Energy Phys. 03 (2015) 003.
[36] L. Calibbi, I. Galon, A. Masiero, P. Paradisi, and Y. Shadmi, Charged slepton flavor post the 8 TeV LHC: A simplified model analysis of low-energy constraints and LHC SUSY searches, J. High Energy Phys. 10 (2015) 043.
[37] K. Kowalska, L. Roszkowski, E. M. Sessolo, and A. J. Williams, GUT-inspired SUSY and the muon $g-2$ anomaly: Prospects for LHC 14 TeV, J. High Energy Phys. 06 (2015) 020.
[38] F. Wang, W. Wang, and J. M. Yang, Reconcile muon $g-2$ anomaly with LHC data in SUGRA with generalized gravity mediation, J. High Energy Phys. 06 (2015) 079.
[39] J. Kawamura and Y. Omura, Study of dark matter physics in nonuniversal gaugino mass scenario, J. High Energy Phys. 08 (2017) 072.
[40] A. Corsetti and P. Nath, Gaugino mass nonuniversality and dark matter in SUGRA, strings and D-brane models, Phys. Rev. D **64**, 125010 (2001).
[41] S. F. King, J. P. Roberts, and D. P. Roy, Natural dark matter in SUSY GUTs with nonuniversal gaugino masses, J. High Energy Phys. 10 (2007) 106.
[42] U. Chattopadhyay, D. Das, and D. P. Roy, Mixed neutralino dark matter in nonuniversal gaugino mass models, Phys. Rev. D **79**, 095013 (2009).
[43] B. Ananthanarayan and P. N. Pandita, Sparticle mass spectrum in grand unified theories, Int. J. Mod. Phys. A **22**, 3229 (2007).
[44] S. Bhattacharya, A. Datta, and B. Mukhopadhyaya, Nonuniversal gaugino masses: A signal-based analysis for the Large Hadron Collider, J. High Energy Phys. 10 (2007) 080.
[45] S. P. Martin, Nonuniversal gaugino masses from nonsinglet F terms in nonminimal unified models, Phys. Rev. D **79**, 095019 (2009).
[46] S. P. Martin, Nonuniversal gaugino masses and seminatural supersymmetry in view of the Higgs boson discovery, Phys. Rev. D **89**, 035011 (2014).
[47] A. Anandakrishnan and S. Raby, Yukawa Unification Predictions with Effective "Mirage" Mediation, Phys. Rev. Lett. **111**, 211801 (2013).
[48] M. A. Ajaib, SU(5) with nonuniversal gaugino masses, Int. J. Mod. Phys. A **33**, 1850032 (2018).
[49] M. Dimou, S. F. King, and C. Luhn, Approaching minimal flavor violation from an $SU(5) \times S4 \times U(1)$ SUSY GUT, J. High Energy Phys. 02 (2016) 118.
[50] M. Dimou, S. F. King, and C. Luhn, Phenomenological implications of an $SU(5) \times S4 \times U(1)$ SUSY GUT of flavor, Phys. Rev. D **93**, 075026 (2016).
[51] B. D. Callen and R. R. Volkas, Large lepton mixing angles from a $4+1$-dimensional $SU(5) \times A(4)$ domain-wall braneworld model, Phys. Rev. D **86**, 056007 (2012).
[52] S. Antusch, S. F. King, and M. Spinrath, Spontaneous CP violation in $A_4 \times SU(5)$ with constrained sequential dominance 2, Phys. Rev. D **87**, 096018 (2013).
[53] I. K. Cooper, S. F. King, and C. Luhn, $A_4 \times SU(5)$ SUSY GUT of flavor with trimaximal neutrino mixing, J. High Energy Phys. 06 (2012) 130.
[54] I. K. Cooper, S. F. King, and C. Luhn, SUSY SU(5) with singlet plus adjoint matter and A_4 family symmetry, Phys. Lett. B **690**, 396 (2010).
[55] F. Björkeroth, F. J. de Anda, I. de Medeiros Varzielas, and S. F. King, Towards a complete $A_4 \times SU(5)$ SUSY GUT, J. High Energy Phys. 06 (2015) 141.
[56] P. A. R. Ade *et al.* (Planck Collaboration), Planck 2013 results. XVI. Cosmological parameters, Astron. Astrophys. **571**, A16 (2014).
[57] E. Aprile *et al.* (XENON Collaboration), First Dark Matter Search Results from the XENON1T Experiment, Phys. Rev. Lett. **119**, 181301 (2017).
[58] G. Aad *et al.* (ATLAS, CMS Collaboration), Combined Measurement of the Higgs Boson Mass in pp Collisions at $\sqrt{s} = 7$ and 8 TeV with the ATLAS and CMS Experiments, Phys. Rev. Lett. **114**, 191803 (2015).
[59] J. P. Lees *et al.* (*BABAR* Collaboration), Exclusive measurements of $b \to s\gamma$ transition rate and photon energy spectrum, Phys. Rev. D **86**, 052012 (2012).
[60] S. Chatrchyan *et al.* (CMS Collaboration), Measurement of the B(s) to $\mu^+\mu^-$ Branching Fraction and Search for B0 to $\mu^+\mu^-$ with the CMS Experiment, Phys. Rev. Lett. **111**, 101804 (2013).
[61] W. Porod, SPheno, a program for calculating supersymmetric spectra, SUSY particle decays and SUSY particle production at e^+e^- colliders, Comput. Phys. Commun. **153**, 275 (2003).
[62] W. Porod and F. Staub, SPheno 3.1: Extensions including flavor, CP phases and models beyond the MSSM, Comput. Phys. Commun. **183**, 2458 (2012).
[63] G. Belanger, F. Boudjema, A. Pukhov, and A. Semenov, micrOMEGAs_3: A program for calculating dark matter observables, Comput. Phys. Commun. **185**, 960 (2014).
[64] G. Pasztor, Search for gauginos and gauge mediated SUSY breaking scenarios at LEP, *Proc. Sci.*, HEP20052006 (2006) 346 [arXiv:hep-ex/0512054].

[65] D. Dercks, N. Desai, J. S. Kim, K. Rolbiecki, J. Tattersall, and T. Weber, CheckMATE 2: From the model to the limit, Comput. Phys. Commun. **221**, 383 (2017).

[66] J. Alwall, R. Frederix, S. Frixione, V. Hirschi, F. Maltoni, O. Mattelaer, H.-S. Shao, T. Stelzer, P. Torrielli, and M. Zaro, The automated computation of tree-level and next-to-leading order differential cross sections, and their matching to parton shower simulations, J. High Energy Phys. 07 (2014) 079.

[67] T. Sjostrand, S. Mrenna, and P. Z. Skands, A brief introduction to PYTHIA 8.1, Comput. Phys. Commun. **178**, 852 (2008).

[68] J. de Favereau, C. Delaere, P. Demin, A. Giammanco, V. Lemaitre, A. Mertens, and M. Selvaggi (DELPHES 3 Collaboration), A modular framework for fast simulation of a generic collider experiment, J. High Energy Phys. 02 (2014) 057.

[69] G. Aad *et al.* (ATLAS Collaboration), Search for direct production of charginos and neutralinos in events with three leptons and missing transverse momentum in $\sqrt{s} = 8$ TeV pp collisions with the ATLAS detector, J. High Energy Phys. 04 (2014) 169.

[70] ATLAS Collaboration, Search for supersymmetry with two and three leptons and missing transverse momentum in the final state at $\sqrt{s} = 13$ TeV with the ATLAS detector, CERN Report No. ATLAS-CONF-2016-096, 2016.